Measurement of Phase Coherence during the Growth of an Elongated Condensate

Mathilde Hugbart, Jocelyn A. Retter, Andres Varòn, Philippe Bouyer, Alain Aspect

Measurement of Phase Coherence during the Growth of an Elongated Condensate

M. Hugbart, J. A. Retter,* A. F. Varón, P. Bouyer, and A. Aspect
Laboratoire Charles Fabry de l'Institut d'Optique,
UMR8501 du CNRS, 91403 Orsay Cedex, France.
(Dated: February 15, 2006)

We study the growth of an elongated condensate from a non-equilibrium thermal cloud obtained by shock-cooling. Quantitative measurements using momentum Bragg spectroscopy reveal the evolution of the phase coherence length as the condensate grows to equilibrium. A broadening of the momentum distribution compared to that expected at equilibrium is observed at early times. This broadening is compatible with damped quadrupole oscillations.

PACS numbers: 03.75.Kk,03.75.Nt

The non-equilibrium path to Bose-Einstein condensation is a complex process, by which atoms accumulate in the ground state of the system, and long-range phase coherence develops, resulting in a strong suppression of density fluctuations and a uniform phase. The kinetics of condensate formation has long been a subject of theoretical study, giving rise to various predictions (see [1] for a review). Quantitative theories have been formulated to model the condensate formation process in a harmonic trapping potential [2, 3]. However, in these models the growing condensate is always assumed to be fully phase coherent. On the other hand, for a homogeneous system, Kagan *et al.* [4] proposed the appearance of a quasi-condensate with strong phase fluctuations which die out on a time scale that increases with the size of the system. This homogeneous system description is also relevant to condensate growth in hydrodynamic clouds, where the trapping potential can be neglected [5]. Condensates in highly-elongated traps, which can often be treated using the local density approximation, are expected to have properties close to the homogeneous case [6]. In addition, the axially hydrodynamic regime is easily attainable in such traps [7].

Experimentally, the problem of condensate formation has been approached by shock-cooling [8, 9, 10] in harmonic traps: starting from a thermal cloud just above the transition temperature, rapid removal of the most energetic atoms from the trap results in an over-saturated thermal cloud. Subsequent thermalization leads to the growth of the condensate. Measurements of the growth of the condensate fraction in nearly-isotropic traps [8, 9] have obtained good quantitative agreement with theory [9, 11], but these experiments did not give access to the phase coherence of the growing condensate. Although the two-step growth curve reported in Ref. [9], and the growth of non-equilibrium, phase-fluctuating condensates from hydrodynamic clouds in Ref. [10], support the existence of a quasi-condensate during the initial stage of condensate formation as proposed in Ref. [4], there exists to our knowledge no quantitative experimental study of the development of phase coherence.

In this Letter, we present an experimental study of the evolution of phase coherence during the growth of a condensate in a highly elongated trap, in the axially hydrodynamic regime. We use Bragg spectroscopy [12] to measure the momentum distribution, which allows an accurate determination of the coherence length [13]. During the early stages of growth, we observe a broadening of the momentum width which is damped over a few hundred milliseconds. Our observations are compatible with the scenario of Refs. [4, 5], where a non-equilibrium quasi-condensate is created at the onset of condensation and relaxes to equilibrium with shape oscillations.

In our experiment [14], we prepare a thermal cloud of ^{87}Rb atoms in the $5S_{1/2}|F = 1, m_F = -1\rangle$ state in an Ioffe-Pritchard trap with trap frequencies of $\omega_\perp = 2\pi \times 655(4)$ Hz radially and $\omega_z = 2\pi \times 6.53(1)$ Hz axially. The cloud is cooled by forced radio-frequency (rf) evaporation to an effective trap depth of $\varepsilon_\mathrm{i} = 6$ μK, and the rf knife is held for a time varying from 1 s to 12 s. This ensures thermal equilibrium, and allows us to control the atom number N_i in the range 3–9.5$\times 10^5$. The resulting thermal cloud has a temperature T_i of about $\varepsilon_\mathrm{i}/10$, just above the transition temperature T_c, which varies from 400 nK to 600 nK depending on the atom number.

We next shock-cool the cloud by ramping the rf knife rapidly down to a final trap depth $\varepsilon_\mathrm{f} = 1.5$ μK in 25 ms. The relative truncation rate $\dot{\varepsilon}/\varepsilon_\mathrm{f} = 120$ s^{-1} is fast compared to the axial trap frequency, but slow compared to the radial trap frequency. In our elongated geometry this shock-cooling therefore results in a cloud transversally at equilibrium but axially out of equilibrium. The cloud tends towards local thermal equilibrium with a temperature $T < T_\mathrm{c}$, in a time $\sim 3\,\tau_\mathrm{coll} \lesssim 10$ ms [15] where τ_coll is the collision rate at the centre of the trap Since the atom cloud is in the hydrodynamic regime axially ($\omega_z \tau_\mathrm{coll} \ll 1$) [16], global equilibrium is reached on a time scale longer than the axial oscillation period.

In order to study the condensate growth, the cloud is held in the trap for a further time t after the end of the shock-cooling ramp, with the trap depth held constant at ε_f. We then switch off the trap and image the cloud after a 20 ms time-of-flight in order to obtain the total atom number N, temperature T and condensate

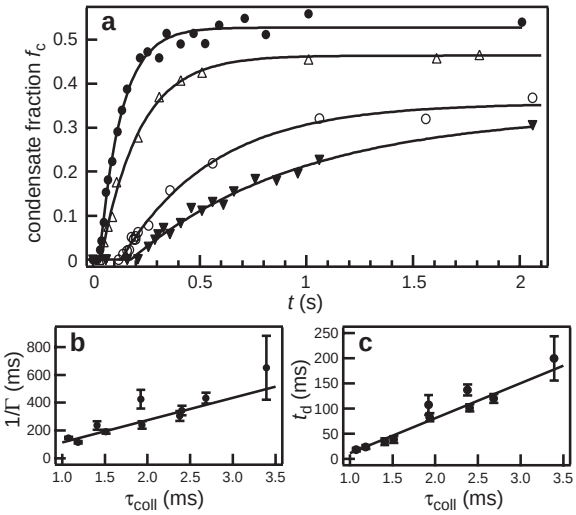

FIG. 1: (a) Growth curves for various initial atom numbers: $N_i/10^5 = 9.5(10)\bullet$, $8.0(8)\triangle$, $3.8(4)\circ$ and $3.1(6)\blacktriangledown$. Each point corresponds to an average over three experimental realizations. (b,c) Values of $1/\Gamma$ and t_d as a function of collision time τ_{coll} in the initial thermal cloud. The fits shown are $1/\Gamma = -46(19) + 160(14)\,\tau_{coll}$ and $t_d = -60(6) + 70(4)\,\tau_{coll}$.

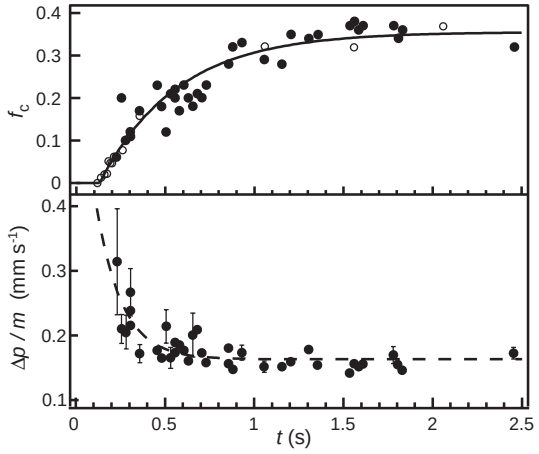

FIG. 2: Condensate fraction f_c and momentum width Δp as a function of t for an initial atom number $N_i = 4.2(3) \times 10^5$. Open circles and solid line represent the data and fit from Fig. 1 for $N_i = 3.8(3) \times 10^5$. The dashed line is a guide to the eye.

fraction f_c [7, 17]. By repeating the measurements at different times t for the same initial conditions, we obtain a growth curve for the condensate fraction, as shown in Fig. 1(a) for various initial atom numbers N_i. At $t \simeq 20$ ms (depending on initial conditions), the atom number has dropped by 40% and the temperature is already below T_c [18], yet the condensate does not appear until a later time. Following the analysis of Ref. [9] we fit the growth curves of Fig. 1(a) with a simple relaxation equation $f_c(t) = H(t - t_d)\; f_c(\infty)\left(1 - e^{-\Gamma(t-t_d)}\right)$, with $H(x)$ the step function. We thereby quantify the delay time t_d before the onset of condensation and the rate of relaxation Γ towards equilibrium. We find that both t_d and $1/\Gamma$ vary linearly with atomic collision time τ_{coll} in the initial thermal cloud, as shown in Fig. 1(b)–(c). The delay time t_d varies from 20 ms to 200 ms before the first appearance of a condensate, corresponding to $t_d \sim 20$–$60\,\tau_{coll}$. The condensate fraction grows to equilibrium with a time constant $1/\Gamma$ varying from 100 ms to 650 ms. The shape of the measured growth curves and the orders of magnitude of t_d and Γ are consistent with the results of previous experiments with nearly-isotropic condensates [8, 9], and with theoretical predictions [2] which do not take phase fluctuations into account. Although we are in a regime where phase fluctuations are always present (see below), we do not observe the two-step growth curve reported in Ref. [9].

We now turn to the experimental study of the phase coherence. We measure the coherence length of the condensate via its momentum distribution, using 4-photon Bragg Spectroscopy as described in Ref. [13]. At time t after the end of the shock-cooling ramp, the magnetic trap is switched off and after 2 ms of free expansion a 2 ms Bragg pulse is applied. The atoms are imaged after a further 16 ms time-of-flight, which allows separation of the diffracted atoms. The diffracted fraction is measured as a function of ν, the detuning between the Bragg beams which determines the velocity-class diffracted, to obtain the momentum spectrum of the condensate. We fit a Lorentzian function to the measured spectra and extract the half-width at half-maximum (HWHM) $\Delta\nu = 2k_L\Delta p/2\pi m$, where m is the atomic mass, k_L the laser wave-vector and Δp the HWHM of the momentum distribution. Each spectrum requires around 50 condensate diffraction measurements, so it takes several weeks to obtain one set of data, such as shown in Fig. 2. For each set, we maintain a constant value of N_i by adjusting the hold time immediately before the shock-cooling ramp. For each spectrum, further images (typically 5) are taken without the Bragg pulses, from which the temperature T, condensate atom number $N_0 = f_c N$, and condensate half-length L are obtained.

The evolution of the momentum width Δp for an initial atom number $N_i = 4.2(3) \times 10^5$ is presented in Fig. 2 (lower panel). The corresponding condensate fractions are shown in the upper panel of Fig. 2 (filled circles). We observe that the momentum width Δp decreases as the condensate fraction grows to equilibrium indicating that, as expected, the coherence length grows with time. We first focus on the value obtained for the momentum width once the condensate reaches equilibrium ($t \gtrsim 1.5$ s). As this experiment is performed in an elongated trapping geometry, temperature-dependent phase-fluctuations can be present even at equilibrium [6, 13, 19, 20, 21]. For our parameters, the phase-coherence length $L_\phi = 15\hbar^2 N_0/16 m k_B L T$ [6] is smaller

than the condensate half-length L by a factor in the range 4–10.As in [13], this entails a broadening of the momentum width, which is given by [6, 22]:

$$\Delta p_{\rm equ} = \hbar \sqrt{\left(\frac{2.04}{L}\right)^2 + \left(\frac{0.65}{L_\phi}\right)^2}. \qquad (1)$$

The first term accounts for the Heisenberg-limited momentum width, due to the finite size L of the condensate; the second term for the presence of the thermal phase fluctuations. The numerical factors account for integration over the 3D density profile. We also correct for the finite "instrumental width" of the Bragg spectrometer, by introducing as in [13] a Gaussian apparatus function of half-width $w_{\rm G} = 200$ Hz. This results in a theoretical measured momentum width:

$$\Delta p_{\rm th} = \frac{\Delta p_{\rm equ}}{2} + \sqrt{\left(\frac{2\pi m}{2k_{\rm L}}\right)^2 w_{\rm G}^2 + \left(\frac{\Delta p_{\rm equ}}{2}\right)^2}. \qquad (2)$$

For $t \gtrsim 1.5$ s, our measurements are in good agreement with the predictions of Equ. 2, though with a systematic excess which we will discuss below (see Fig. 3).

We now focus on earlier times, $t \lesssim 1.5$ s, when the condensate fraction is still increasing. From Equ. 1, we see that even if the condensate were at equilibrium at each moment during the growth, we would expect the momentum width to decrease with time, since both L_ϕ and L increase with the condensate atom number. We take this into account by comparing each measured momentum width Δp with the value $\Delta p_{\rm th}$ calculated from Equ. 2 using the parameters N_0, L and T measured for each Bragg spectrum. We plot the ratio $\Delta p/\Delta p_{\rm th}$ in Fig. 3 for two different initial atom numbers: (a) $N_{\rm i} = 4.2(3) \times 10^5$ and (b) $N_{\rm i} = 8.0(3) \times 10^5$. The error bars shown represent typical statistical errors. The dashed line at $\Delta p/\Delta p_{\rm th} = 1$ indicates the value expected for a condensate always at equilibrium. Systematic uncertainties of 15% on this equilibrium value, mainly due to the atom number calibration (20%) and determination of $w_{\rm G}$ (10%), are represented by the gray band. Unambiguously, we observe that the ratio $\Delta p/\Delta p_{\rm th}$ always lies above one (with values close to one at time as short as 100 ms), and decreases in time. This indicates an excess momentum spread with respect to a condensate at equilibrium during the growth.

This observed excess momentum width with strong measurement dispersion is compatible with the presence of quadrupole shape oscillations of the condensate, similar to those observed in Refs. [10, 13]. Indeed, for a sufficiently high initial atom number ($N_{\rm i} \gtrsim 9 \times 10^5$), we directly observe quadrupole oscillations of the condensate in the absorption images, as shown in Fig. 4 for $N_{\rm i} = 9.5 \times 10^5$. The fitted frequency $\omega_{\rm Q} = 1.56(3)\,\omega_z$ is consistent with the theoretical value, $1.58\,\omega_z$ [23]. The oscillation amplitude is 12 μm at $t = 200$ ms, and decays with a time constant of about 250 ms. These oscillations of the axial condensate length, $L(t) = L(0) + \xi(t)\cos[\omega_{\rm Q}(t - t_{\rm d})]$, where $\xi(t)$ is the decaying amplitude, lead to an excess axial momentum $\Delta p_{\rm osc} = 0.54\, m\omega_{\rm Q}\, \xi(t)\, \left|\sin[\omega_{\rm Q}(t - t_{\rm d})]\right|$. During the acquisition of the Bragg spectra, small variations in the initial atom number and temperature occur, which are expected to lead to fluctuations of $t_{\rm d}$. This dephases the oscillations between different measurements and results in a measurement dispersion, as seen in Fig. 3, rather than clear oscillations. The excess momentum widths in Fig. 3 can be interpreted by assuming oscillations with amplitudes of 4 μm ($N_{\rm i} = 4.2 \times 10^5$) and 5.5 μm ($N_{\rm i} = 8.0 \times 10^5$) [24], which decay with time constants of about 700 ms and 300 ms respectively. These values are consistent with those of Fig. 4, assuming an oscillation

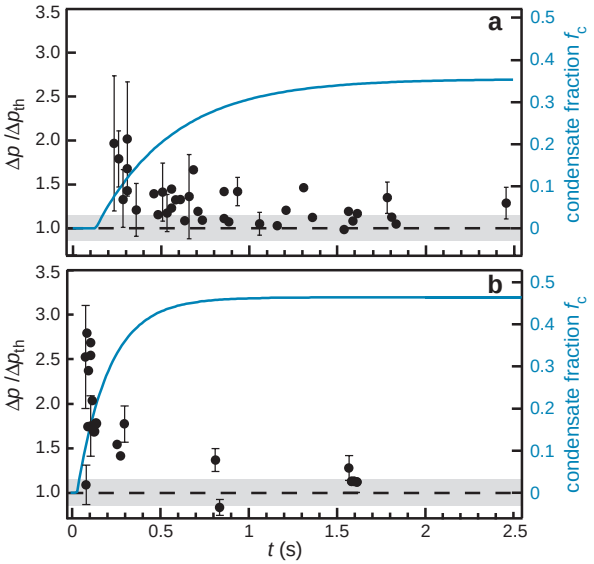

FIG. 3: Ratio of measured momentum width Δp to theoretical momentum width $\Delta p_{\rm th}$, calculated for a condensate at equilibrium (Equ. 2) for: (a) $N_{\rm i} = 4.2(3) \times 10^5$ and (b) $N_{\rm i} = 8.0(3) \times 10^5$. (Data shown in (a) corresponds to Fig. 2.) The condensate momentum width tends to the equilibrium value (dashed line) at long times. Error bars represent statistical error and the gray band the systematic uncertainties. The solid curves (right-hand scale) reproduce growth curve fits from Fig. 1(a).

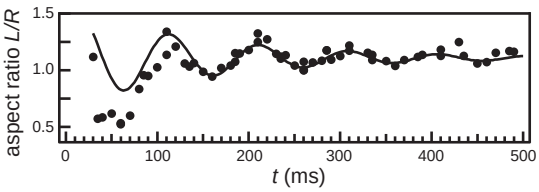

FIG. 4: Quadrupole oscillations during condensate growth, for $N_{\rm i} = 9.5 \times 10^5$, as observed in the aspect ratio of the condensate after time-of-flight. The solid line is a fit to the data.

amplitude which increases with the atom number and a decay time which decreases with the atom number.

This picture is compatible with the scenario of Kagan *et al.* [4], in which, for a homogeneous system three distinct stages are identified during the growth of a condensate. In the first stage, Boltzmann kinetic processes lead to accumulation of atoms in the lowest energy levels: this *kinetic* stage is determined by the collision time $\tau_{\rm coll}$. Secondly, density fluctuations are suppressed during a fast *coherent* stage, resulting in a quasi-condensate with non-equilibrium, long-range phase fluctuations. This stage generally occurs on a time scale much shorter than that of the kinetic stage. During the final stage, phase-fluctuations decay to produce the true phase-coherent condensate, with a characteristic time scale τ_ϕ which increases with the system size L: $\tau_\phi \propto L$ in the collisionless regime and $\tau_\phi \propto L^2$ in the hydrodynamic regime. It should be noted that our trapped system differs from a homogeneous system, but Svistunov [5] points out that this theory can be applied to trapped hydrodynamic clouds, where the trapping potential can be neglected. In this case, the resulting quasi-condensate will be out-of-equilibrium, thereby exciting a breathing mode. Our observations are consistent with this scenario assuming that the measured slowly decaying momentum excess is due to the breathing mode, while the phase fluctuations decay in less than 100 ms and are not observed in the current experiment [25].

In conclusion, we have observed the growth of a condensate in a very elongated trap and have shown that the presence of phase fluctuations does not qualitatively change the shape of the growth curve. In order to obtain information on the development of phase coherence, we have studied the evolution of the momentum width, and compared it to the width expected for a quasi-condensate at equilibrium with the same atom number and temperature. We find a broadening of the momentum distribution, compatible with quadrupole shape oscillations, which decays on a time scale of the order of a few hundred milliseconds. Because an explicit theory for our experimental situation is lacking, the agreement between theory and experiment can only be qualitative and an extension of the model of Ref. [4] to trapped condensates, particularly in this quasi-1D geometry [26], is required. In order to observe the decay of higher-order excited modes, a measurement of the phase coherence length at shorter times is also needed. This seems exceedingly difficult using Bragg spectroscopy, since at short times the condensate fraction is too small to obtain a clear Bragg spectrum. Other techniques might be used instead, such as atom laser correlation measurements [27], combined with single-atom detection [28, 29].

We thank L. Sanchez-Palencia, G. V. Shlyapnikov, M. J. Davis, F. Gerbier, S. Richard and J. H. Thywissen for useful discussions. We acknowledge support from IXSEA (M.H.), the Marie Curie Fellowship Programme (J.R.) and Fundación Mazda para el Arte y la Ciencia (A.V). This work was funded by CNRS, DGA, EU (IST-2001-38863, MRTN-CT-2003-505032), INTAS and ESF (QUDEDIS).

* Electronic address: jocelyn.retter@iota.u-psud.fr

[1] H. T. C. Stoof, J. Low Temp. Phys. **114**, 11 (1999).
[2] C. W. Gardiner, *et al.*, Phys. Rev. Lett **79**, 1793 (1997); M. D. Lee and C. W. Gardiner, Phys. Rev. A **62**, 033606 (2000); M. J. Davis, C. W. Gardiner, and R. J. Ballagh, *ibid* **62**, 063608 (2000).
[3] M.J. Bijlsma, E. Zaremba, and H. T. C. Stoof, Phys. Rev. A **62**, 063609 (2000).
[4] Yu. Kagan, B. V. Svistunov, and G. V. Shlyapnikov, JETP **75**, 387 (1992); Yu. Kagan and B. V. Svistunov, *ibid* **78**, 187 (1994); Yu. Kagan and B. V. Svistunov, Phys. Rev. Lett. **79**, 3331 (1997).
[5] B. Svistunov, Phys. Lett. A **287**, 169 (2001).
[6] D. S. Petrov, G. V. Shlyapnikov, and J. T. M. Walraven, Phys. Rev. Lett. **87**, 050404 (2001).
[7] F. Gerbier *et al*, Phys. Rev. Lett. **92**, 030405 (2004).
[8] H.-J. Miesner *et al.*, Science **279**, 1005 (1998).
[9] M. Köhl, *et al.*, Phys. Rev. Lett. **88**, 080402 (2002).
[10] I. Shvarchuck *et al.*, Phys. Rev. Lett **89**, 270404 (2002).
[11] M. J. Davis and C. W. Gardiner, J. Phys. B **35**, 733 (2002).
[12] J. Stenger *et al.*, Phys. Rev. Lett. **82**, 4569 (1999).
[13] S. Richard, *et al.*, Phys. Rev. Lett. **91**, 010405 (2003).
[14] B. Desruelle *et al*, Phys. Rev. A **60**, R1759 (1999).
[15] C. R. Monroe *et al.*, Phys. Rev. Lett. **70**, 414 (1993); H. Wu and C. J. Foot, J. Phys. B **29**, L321 (1996).
[16] For the thermal cloud immediately before the shock-cooling ramp, we obtain $0.04 < \omega_z \tau_{\rm coll} < 0.13$.
[17] F. Gerbier *et al*, Phys. Rev. A **70**, 013607 (2004).
[18] The atom number and temperature continue to fall slowly during t due to the constant rf knife.
[19] S. Dettmer *et al.*, Phys. Rev. Lett. **87**, 160406 (2001).
[20] D. Hellweg *et al.*, Phys. Rev. Lett. **91**, 010406 (2003).
[21] M. Hugbart *et al.*, Eur. Phys. J. D **35**, 155 (2005).
[22] F. Gerbier *et al.*, Phys. Rev. A **67**, 051602 (2003).
[23] S. Stringari, Phys. Rev. Lett. **77**, 2360 (1996).
[24] For such small amplitudes, the oscillations cannot be directly observed in the time-of-flight images due to the limited resolution of our imaging system.
[25] With our experimental numbers, we calculate from [4] a damping time τ_ϕ between 10 ms and 500 ms, depending on the collisional regime..
[26] N. P. Proukakis, J. Schmiedmayer, and H. T. C. Stoof, cond-mat/0509154 (2005).
[27] I. Bloch, T. W. Hänsch, and T. Esslinger, Nature **403**, 166 (2000).
[28] A. Öttl, S. Ritter, M. Köhl, and T. Esslinger, Phys. Rev. Lett. **95**, 090404 (2005).
[29] M. Schellekens, *et al.* Science, **310**, 648 (2005).